

RECENT LASER GUIDED TRANSPORT CALCULATIONS *

J.K.Boyd

Lawrence Livermore National Laboratory

P.O.Box 808 Livermore, CA 94550

Abstract

Laser guided transport has been simulated in axisymmetry for intense electron beams at energies ranging from 3 to 45 MeV for currents of 2 to 5 kA. The simulation includes time variation of guiding channel formation and the time evolution of channel ion oscillations. Experimental behavior is also predicted with less elaborate beam slice calculations and the beam envelope model. Examples are presented of various channel focusing strengths and ratio of beam to channel radius.

1. Introduction

A relativistic electron beam can be focused and transported by a channel of ions. The behavior of the electrons transported by an ion channel is fundamentally different compared to magnetic transport for two reasons. First, the radial potential depends strongly on the position of an electron with respect to the edge of the channel. Second, transport properties depend strongly on the density and spatial profile of the ion channel. Furthermore the ion channel is also affected by its formation process. Among the various methods of channel formation, usually impact or photo ionization is used. In the ATA experiment a laser is used to ionize a background gas and generate an ion channel which is similar to the spatial profile of the laser. This process is known as laser guided transport [1].

The ATA electron beam is created in a diode gap. Since it is not possible to have the level of background gas needed for laser guided transport in the diode, it is necessary to begin transport using magnetic focusing. The implication of this necessity is that there must be a transition from magnetic to laser guided transport. The complexity of this process coupled with the previously mentioned considerations has required extensive numerical modeling. Many computer runs have been done in the axisymmetric approximation with either an envelope beam model or the more complete DPC [2] simulation.

The basic beam behavior particular to the laser guiding transport technique is discussed in section 2. Attention is given to the consequence of ion motion and what this means for various parameter relationships. In section 3 the results of envelope calculations are presented for typical ATA parameters. In the low current regime the initial conditions for envelope calculations are obtained from DPC calculations that model beams for FEL applications. The DPC ion channel model and additional ATA results are discussed in section 4. The emittance growth results for several operational conditions are presented in the context of the most likely $m = 0$ mode driver. This was originally thought to be based on the disparity of the ion channel size seen by early and late parts of the beam pulse.

2. Basic Beam Behavior with Laser Guiding

The ATA beam is transported by an ion channel focusing force. The channel is formed by ionization caused by a laser passing through benzene. The laser initially produces a plasma and thus the plasma electrons are usually assumed to be expelled by the passage of the intense relativistic electron beam. The process of ionization and the expulsion of plasma electrons each occur in a finite amount of time. At a fixed z position the ion density builds up in accordance with an ionization rate equation. During buildup plasma electrons are being expelled and ions experience the radial field of the relativistic electrons. The ions are then attracted toward the axis until their own charge density increase repels them to a larger radius. With a sufficiently long beam pulse the ions oscillate in the electric field of the beam. In typical ATA operation ions collapse toward the axis and just begin to expand during the time of a pulse.

The relativistic electron beam which is being guided by the ion channel does not experience a fixed focusing force. The focusing force varies in τ (where τ is the time back from the beam head) due to the deposition time of the ions, the collapse of the ions toward the axis, and interaction with plasma electrons. There are also other τ dependent effects such as charge exchange, cracking of benzene into fragments and beam induced ionization which complicate this picture.

Much of the basic beam behavior with laser guiding can be understood approximately using models which ignore z variation. Clearly these models do not explain phenomena near gaps, or the beam head and tail. They

apply only in the body of the beam. The main purpose in studying these models is to provide indications of behavior which augment the process of understanding the experimental data. Conclusions drawn from these models can provide intuition about what is occurring at the beam head and tail, but do not lead to definitive information in this region. More complete information is obtained from the more elaborate DPC calculations.

Plasma electron expulsion

One of the substantial questions is whether or not the plasma electrons are actually expelled. Some plasma electrons must be expelled in order that the beam is guided, but perhaps not all. Since the beam has a strong pinch force and the channel attracts electrons, in some circumstances plasma electrons accelerate and join the beam electrons which originated from the injector. An answer can be obtained by solving the radial and axial equations of motion. (assume no angular momentum)

$$\begin{aligned} \frac{d\beta_r}{dt} &= -\frac{qE_r}{\gamma mc} \beta_r^2 + \frac{q}{\gamma mc} (E_r - \beta_z B_\theta) \\ \frac{d\beta_z}{dt} &= -\frac{qE_r}{\gamma mc} \beta_r \beta_z + \frac{q}{\gamma mc} \beta_r B_\theta \end{aligned}$$

This is the approach employed by DPC, but including all the force equation terms. The solution of these equations gives a detailed description of electron trajectories, but is more than necessary to determine if plasma electrons hit the wall.

In the main body of the pulse z variation is small and can be ignored. In the approximation of a long pulse with no z variation, the Hamiltonian can be used to determine whether or not plasma electrons are expelled. When there is no E_z field the canonical momentum, \mathcal{P}_z is conserved. (Obviously this does not apply near a gap!) The normalized relativistic Hamiltonian is then,

$$\mathcal{H} = \left(\frac{1}{4} + \frac{\mathcal{P}_r^2}{4m^2c^2} + \frac{(\mathcal{P}_\theta - \frac{q}{c}A_\theta)^2}{(2mcr)^2} + \frac{(\mathcal{P}_{z0} - \frac{q}{c}A_z)^2}{4m^2c^2} \right)^{\frac{1}{2}} + \frac{q}{2mc^2} \phi \quad (1)$$

Since the channel plasma electrons are assumed to be birthed at rest with no magnetic field the \mathcal{P}_θ term of Eq.(1) will be excluded in the following analysis. (In a transition region from magnetics to laser guiding it must be included.) Because \mathcal{H} is conserved, and a plasma electron is initially at rest, Eq.(1) can be rearranged to express \mathcal{P}_r^2 only in terms of a function of r and initial quantities (denoted by subscript 0).

$$\frac{1}{4m^2c^2} \mathcal{P}_r^2 = \left(\frac{q}{2mc^2} (\phi_0 - \phi) + \frac{1}{2} \right)^2 - \frac{1}{4} - \frac{1}{4m^2c^2} (\mathcal{P}_{z0} - \frac{q}{c}A_z)^2 \quad (2)$$

The left side of Eq.(2) is manifestly positive definite and thus all allowed radial positions must satisfy,

$$\left(\frac{q}{2mc^2} (\phi_0 - \phi) + \frac{1}{2} \right)^2 - \frac{1}{4} - \frac{1}{4m^2c^2} (\mathcal{P}_{z0} - \frac{q}{c}A_z)^2 > 0 \quad (3)$$

This condition can be made more precise by expressing A_z in terms of the beam current and ϕ in terms of ion line density. Assuming beam current, $J_b = -(mc^3/e)(\hat{I}/\pi R^2)e^{-r^2/R^2}$, and a gaussian profile for ion density $\rho_i = (mc^2/e)(\hat{\lambda}_i/\pi R_i^2)e^{-r^2/R_i^2}$ with $\hat{I} = |J_b|(e/mc^3)$, $\hat{\lambda} = \lambda_i(e/mc^2)$, and defining the function Q ,

$$Q(r, r_0, R) = \int_{r_0/R}^{r/R} \frac{1 - e^{-x^2}}{x} dx \quad (4)$$

then substituting into Eq.(3) gives,

$$\left[\hat{I}Q(r, r_0, R) - \hat{\lambda}_i Q(r, r_0, R_i) + \frac{1}{2} \right]^2 - \frac{1}{4} - [\hat{I}Q(r, r_0, R)]^2 > 0 \quad (5)$$

For a specified beam current and ion channel line density the only factor in Eq.(5) which can vary is the Q function. From the initial position of an electron to a radius of the size of standard beam pipes Q generally has a range of about 0 to 3. The maximum radius of a plasma electron trajectory is determined when the expression on the left side of Eq.(5) equals zero. If the maximum radius is greater than the wall radius the plasma electron is expelled.

* Performed jointly under the auspices of the USDOE by LLNL under W-7405-ENG-48 and for the DOD under SDIO/SDC-ATC MIPR No. W31RPD-8-D5005.

Ion channel collapse time

A primary postulated cause of emittance variation throughout a beam pulse is the varying focusing force caused by the relationship of beam to ion channel size. For a particular beam radius the focusing force is larger if the ion channel is inside. It is thus important to know the time to minimum ion channel size compared to the time length of the beam pulse. This is especially crucial if the ion channel undergoes several oscillations during the beam pulse.

The time for the collapse of the ions to their minimum radius can be estimated from an electrostatic model. The equation of motion of an ion at the channel edge can be solved assuming only a radial electric field. The governing field equation is,

$$\nabla \cdot \vec{E} = 4\pi\rho_b + 4\pi\rho_i \quad (6)$$

where ρ_b and ρ_i are the beam and channel density. Temporarily assuming no z variation, and flat profiles of beam radius a and channel radius R_i ,

$$\frac{1}{r} \frac{\partial}{\partial r} r E_r = -\frac{4I_b}{10a^2} + \frac{4\lambda_i}{R_i^2} \quad (7)$$

The radial ion channel equation of motion is then,

$$\frac{d^2 r}{dt^2} = \frac{q}{m_i} \left(\frac{2\lambda}{r} - \frac{I_b}{5a^2} r \right) \quad (8)$$

Equation (8) can be multiplied by dr/dt to obtain an expression for the velocity.

$$\frac{dr}{dt} = -\sqrt{\frac{q}{m_i}} \left(4\lambda_i \ln \frac{r}{R_i} - \frac{I_b}{5a^2} (r^2 - R_i^2) \right)^{\frac{1}{2}} \quad (9)$$

which then determines the radial position of minimum radius, r_{min} from $dr/dt = 0$. The estimate of time to collapse to r_{min} is obtained from a solution of Eq.(9).

$$t_{collapse} = -\sqrt{\frac{m_i}{q}} \int_{R_i}^{r_{min}} \frac{dr}{\sqrt{4\lambda_i \ln \frac{r}{a} - \frac{I_b}{5a^2} (r^2 - a^2)}} \quad (10)$$

For typical FEL parameters of $\lambda \sim 60$ esu/cm, $a \sim 1$ cm, $I_b \sim 2500$ amps, $m_i \sim 78$ (benzene), Eq.(10) gives $r_{min} \sim .1383$ cm and $t_{collapse} \sim 50$ ns. At 10^4 amps the time to r_{min} clearly decreases.

3. Envelope Formulation Results

In the envelope formulation reliance is placed on the assumption that plasma electrons are fully expelled. Then it is only necessary to account for the additional force due to an ion channel in the expression for the radial force on the beam. The envelope equation which is used is adapted from a treatment without an ion channel [3],

$$\frac{d^2 R}{dz^2} + \frac{1}{\gamma} \frac{d\gamma}{dz} \frac{dR}{dz} + \frac{U}{R(\beta c)^2} + \frac{k_c^2}{4} R - \frac{E^2}{\gamma^2 R^3} = 0 \quad (11)$$

where $k_c = qB/(\gamma mc^2)$, and $E^2 = (P_\theta/mc)^2 + \gamma^2 R^2 (V^2 - (dr/dz)^2 c^2 - (L/R)^2)/c^2$. To allow for an ion channel the U term is modified with an additional term caused by the radial electric field of the ion channel. For a Gaussian profile the additional term depends on ion line density λ_i , channel radius R_i and the rms beam radius R .

$$U = -\frac{qI_b}{\gamma^3 m \beta c} - \frac{2q\lambda_i}{\gamma m} \frac{R^2}{R^2 + R_i^2} \quad (12)$$

As mentioned earlier an item of concern is the possible growth of emittance as transport proceeds using laser guiding. Such growth is much more likely if the beam has large radial oscillations. In the configuration of ATA the background gas is fed into the beam line at stations that alternate with vacuum pumps. This arrangement enforces some degree of variation of focusing strength with distance. To study this issue the envelope equation has been solved with a channel line density that alternately increases and decreases with distance down the accelerator. In Fig. 1 for $R_i = 0.5$ cm, λ_i varies linearly from 10 to 60 esu/cm, with the high value occurring at the gas input location and the low value at the pumping station. The energy of the beam is increased by 0.25 MV gaps that give an effective gradient of 1 MV/m. A decreasing major oscillation of about a 7 m wavelength is observed. In Fig. 2 the variation of λ_i is 10 times greater, going from 1 to 60 esu/cm. In this extreme example the radial oscillation becomes unstable and grows in amplitude with distance down the accelerator.

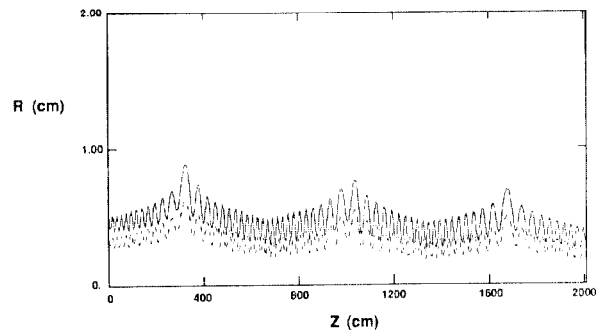


Figure 1. $R(z)$ for a λ_i variation of 10 to 60 esu/cm.

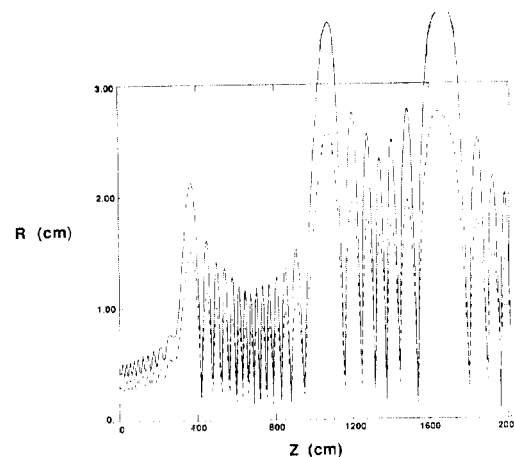


Figure 2. $R(z)$ for a λ_i variation of 1 to 60 esu/cm.

4. DPC Model and Results

The axisymmetric DPC code has been used to simulate laser guided transport for a complete pulse the entire length of ATA. The ion channel responsible for focusing the beam is modeled by particles that are self consistently evolved with the electron beam particles. The formation of the channel ions and their paired plasma electrons is determined by rate equations for laser ionization, and relativistic electron beam background ionization. For each mechanism an appropriate ion mass spectrum is used. As a result the ions undergo considerable radial mixing as they respond to the pinching effect of the relativistic electrons because the collapse time scales like $\sqrt{m_i}$.

The calculation begins at the cathode assuming space charge limited emission and a hyperbolic tangent rise on the anode electrode voltage of the ATA diode configuration. The electron beam is transported magnetically through the ATA injector for reasons described earlier. The evolution of the beam pulse charge density for an example of parameters given in Table 1, is shown in Fig. 3 at $t = 15.5$ ns and $t = 33$ ns. The beam dynamics are appreciably different at different times at the same z location since the energy increases consistent with the anode voltage rise. Subsequent to the injector the beam is focused into a 1 cm radius collimator over which the magnetic field is linearly reduced and the background gas pressure is linearly increased. The beam current, radius, and emittance as a function of time are shown in Fig. 4 at the end of the collimator. The emittance increases back into the pulse, however the radius is slightly decreasing for $t > 20$ ns where there is substantial current. The radius of the ion channel corresponding to Fig. 4 has a minimum situated at 48 ns. Approximately 3 m further downstream similar plots are shown in Fig. 5 after the beam traverses 5 gaps and increases energy by 1.25 MV. At this location the emittance has

Table 1. ATA parameters.

Diode voltage	3.0 MV
Voltage rise time	20.0 ns
A-K gap	13.0 cm
Cathode radius	6.8 cm
Pipe radius	6.8 cm
λ_i	60 esu/cm
Collimator radius	1.0 cm

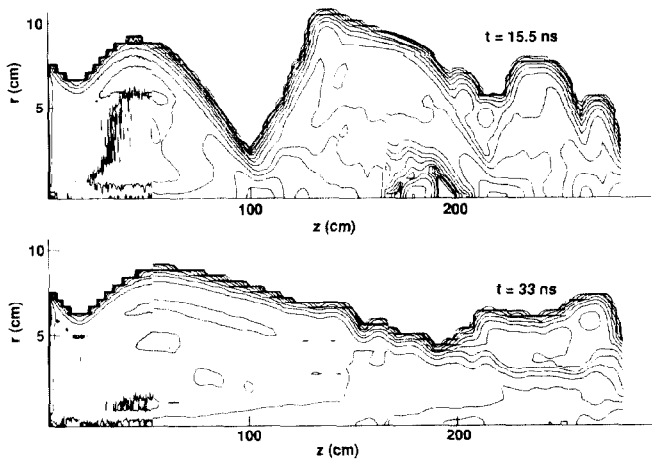


Figure 3. ATA charge density at $t = 15$ and 33 ns.

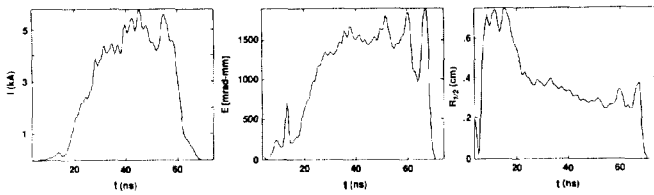


Figure 4. End of collimator current, emittance and radius.

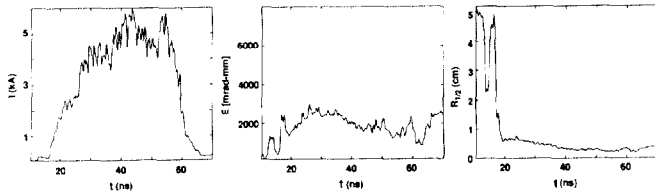


Figure 5. ATA current, emittance and radius after 5 gaps of acceleration.

increased by about 30% and the radius decreases slightly. Because the early part of the beam begins the collapse of the ion channel, a major question is whether or not a particular section of beam encounters an invariant focusing force. The bulk force is the same if the channel radius seen by the beam is constant. By following beam particles at the front of the pulse and near the beam "time" at which the ion channel collapses to a minimum, it can be seen in Fig. 6 that the ion channel is approximately constant. Notice however that the early part of the beam sees a channel of roughly three times the radius as the later part. In each instance the beam radius and channel radius are approximately the same size. Further down the accelerator the electron beam tends to be inside the ion channel radius since the equilibrium radius of the beam decreases as energy increases. At the end of the accelerator in Fig. 7 the current, radius and emittance are compared to that exiting the collimator for a lower current case. The beam radius decreases by a factor of two and the emittance increases by about 60%.

5. Summary

Expressions have been derived which determine when electrons are captured in a simple z independent model. In the same approximation, ignoring the spectrum of ion masses the ion collapse time has been calculated. For typical ATA currents of 2 to 5 kA the collapse occurs near the end of the pulse. Thus any adverse emittance growth effects caused by ion collapse would be expected near the end of the pulse.

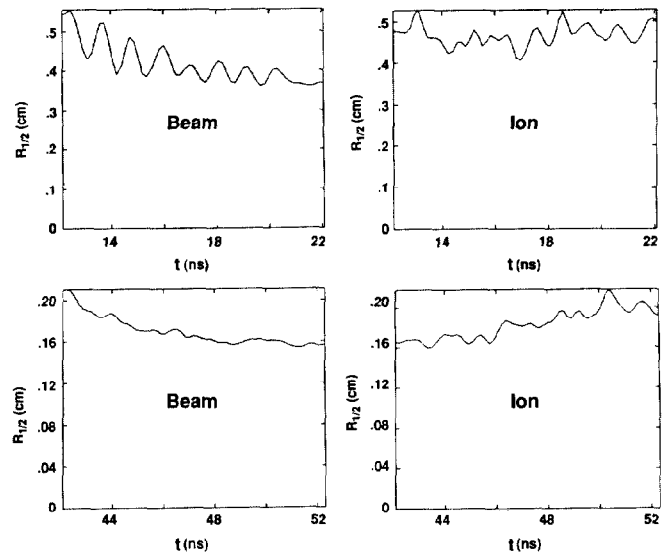


Figure 6. ATA beam and ion radius for two pulse times.

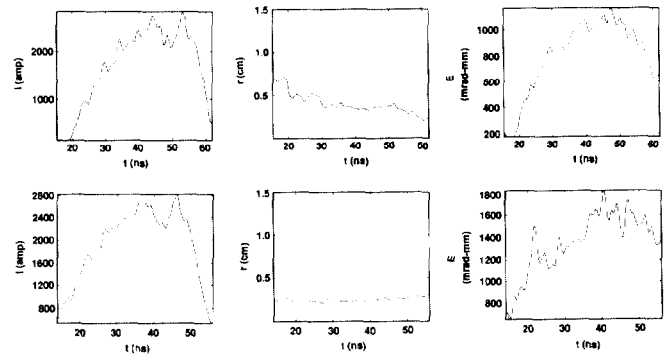


Figure 7. End of ATA I, R, and E compared to the collimator result.

The occurrence of unstable radial oscillations has been demonstrated for extreme ion channel λ_i variation. The mechanism for this variation is realistic, however it is experimentally possible to prevent the degree of variation which can be troublesome.

The DPC code has been used to simulate laser guided transport for a complete pulse the entire length of ATA. The variation of channel radius throughout the beam pulse has been confirmed and emittance growth has been demonstrated at the end of the ATA accelerator. It has been shown the ion channel focusing force is different at the front and back of the beam pulse however the focusing force tends to be approximately the same as seen by each of these sections of the total pulse.

REFERENCES

- [1] G.J. Caporaso, F. Rainer, W.E. Martin, D.S. Prono, A.G. Cole, *Phys. Rev. Lett.* **15** (13), 1591 (1986).
- [2] J.K. Boyd, Proc. Seventh Int. Conf. on Free Electron Lasers, Tahoe City, USA, Sept. (1985), p. 87.
- [3] E.P. Lee and R.K. Cooper, *Part. Accel.* **7**, 83 (1976).